Article

Piezoelectric Nanogenerator Based on Electrospun Cellulose Acetate/Nanocellulose Crystal Composite Membranes for Energy Harvesting Application

SUN Bolun, CHAO Danming and WANG Ce✉

Received June 22, 2021
Accepted August 20, 2021

Nanogenerators, as the typical conversion of mechanical energy to electrical energy devices, have great potential in the application of providing sustainable energy sources for powering miniature devices. In this work, cellulose acetate/cellulose nanocrystal(CA/CNC) composite nanofiber membranes were prepared by electrospinning method and then utilized to manufacture a flexible pressure-driven nanogenerator. The addition of CNC not only increased the content of piezoelectric cellulose I crystallization but also strengthened the mechanical deformation of the nanofiber membranes, which could greatly enhance the piezoelectric performance of CA/CNC composite membranes. The CA/CNC composite nanofiber membrane with 20%(mass fraction) of CNC(CA/CNC-20%) showed optimal piezoelectric conversion performance with the output voltage of 1.2 V under the force of 5 N(frequency of 2 Hz). Furthermore, the output voltage of the CA/CNC-20% nanogenerator device exhibited a linear relationship with applied impact force, indicating the great potential in pressure sensors.

Keywords Piezoelectric; Nanogenerator; Electrospinning; Cellulose acetate; Nanocellulose crystal

1 Introduction

Driven by the growing demand for clean energy and the development of portable miniature devices, eco-friendly energy technologies, and novel materials, which could harvest energy from the surrounding environment, including solar energy, wind, ocean wave, and mechanical energy have attracted much exploration in recent decades[1—4]. Among these, some mechanical energies in nature and the living environment, such as mechanical vibration, sound waves, and body movement, have been considered as potential renewable power sources[5,6]. However, due to the wide distribution and the small energy density(milli to tens of watts), these small kinetic energies are difficult to be harvested for conventional electric generators but are possible for nanogenerators[7—9]. Multiple nanogenerators based on piezoelectric effect[10,11], pyroelectric effect[12,13], and triboelectric effect[14—16] have been invented and applied to converting ambient environmental energy into useful electrical power. Among them, piezoelectric nanogenerators fabricated by piezoelectric materials with micro- or nano-structures have attracted significant attention due to their portability, sustainability, simple structure, and wide application environment[17—19].

So far, piezoelectric materials can be broadly divided into two types: inorganic and organic materials. Inorganic piezoelectric crystals and ceramics, such as ZnO[20,21], $Pb(Zr_xTi_{1-x})O_3$[22,23], and $BaTiO_3$[24,25] have been widely used to fabricate piezoelectric nanogenerators with good performance. Although organic materials cannot provide high-performance piezoelectric properties like inorganic stuff, they still attract great interest to researchers due to their lightweight, flexibility, and property tunability *via* multifarious chemical reactions. Recently, polyvinylidene fluoride and its derivatives, as the representatives of organic piezoelectric materials[26,27], have been continually prepared and reported as piezoelectric nanogenerators. For a better understanding of the organic piezoelectric mechanism and expansion of practical applicability, multifunctional organic piezoelectric materials, especially flexibility, biocompatibility, and degradability, need to be further explored[28,29].

Cellulose is an emerging piezoelectric polymer featuring renewability and biocompatibility, which endows its low cost and possibility of power sources for wearable/implantable devices[30,31]. Highly ordered hydrogen-bond networks in crystalline cellulose, which induces the asymmetric crystalline structure and permanent dipole moments, are the most important origin of piezoelectricity in cellulose[32]. Native cellulose in plant fibers and wood has a small piezoelectric constant(less than 0.3 pm/V) because of the lignocellulose matrix, mainly due to the random, heterogeneous distribution and a relatively small amount of crystalline cellulose[30,33]. Recently, strong piezoelectric responses were disclosed in nanocellulose materials, such as cellulose nanofibril(CNF)[34,35] and cellulose nanocrystals(CNCs)[36,37], which have been widely exploited in nanogenerators[38–40]. In particular, theoretical calculation of the hydrogen bonds in the unit cell structure suggested that CNCs may possess a piezoelectric coefficient as high as 4—36 pm/V,

✉ WANG Ce
cwang@jlu.edu.cn
Alan G. MacDiarmid Institute, Jilin University, Changchun 130012, P. R. China

https://doi.org/10.1007/s40242-021-1252-x

which is comparable to commercial piezoelectric materials[34]. Wang's group[41] reported a piezoelectric nanogenerator based on vertically aligned cellulose nanocrystal with a large piezoelectric coefficient[(19.3±2.9) pm/V]. Hänninen *et al.*[42] reported a nanogenerator based on nanocellulose and chitosan films by solvent casting method. Nanocellulose materials have shown great potential in energy conversion devices with advantages of low cost, renewability, and promising piezoelectric performance.

In this work, we prepared cellulose acetate/cellulose nanocrystal(CA/CNC) composite nanofiber membranes by the electrospinning technique. The morphology and structure were characterized by scanning electron microscopy, infrared spectra, and X-ray diffraction. Moreover, a piezoelectric nanogenerator device manufactured based on CA/CNC composite nanofiber membrane was investigated in detail.

2 Experimental

2.1 Materials

Cellulose acetate(CA) powder was purchased from Aladdin Industrial Corporation. Nanocellulose crystals(CNC) powder was purchased from North Century(Jiangsu) Cellulose Material Co., Ltd.(Xuzhou, China). *N*,*N*′-Dimethylacetamide(DMAc) and acetone were obtained from Beijing Chemical Factory(Beijing, China). All materials were used as received without any purification.

2.2 Preparation of Nanofibers

CA powder was dissolved in a DMAc-acetone mixed solvent (1:2, volume ratio) by stirring at 25 °C for 6 h. The CA content of the resultant solution was fixed at 18%(mass fraction). Precalculated quantity of CNC powder was added to the CA solution by stirring for another 3 h, and then ultrasonicated for 60 min to obtain a homogeneous solution.

The as-prepared solutions were transferred into a 10 mL plastic syringe. To avoid the deposition of nanoparticles, a small amount of the solution was added to the plastic syringe at a time. The steel needle(tip-diameter 0.8 mm) of the syringe was connected to the positive electrode of a high-voltage DC power supply. Electrospinning was carried out at 15 kV with a feed speed of 1 mL/h. The nanofiber membranes were collected on the aluminum foil covered on a rotating drum(diameter of 20 cm) with a rotating speed of 200 r/min. The aluminum foil collector was placed 20 cm away from the needle and was connected to a negative voltage of –1 kV. All the electrospun nanofibrous mats were dried under vacuum at 60 °C overnight. Four kinds of CA/CNC nanocomposites with diverse CNC contents of 5%, 10%, 15%, 20%(mass fraction) were fabricated and defined as CA/CNC-5%, CA/CNC-10%, CA/CNC-15%, and CA/CNC-20%, respectively. For comparison, a neat CA nanofibrous membrane was also prepared in a similar procedure.

2.3 Fabrication of Piezoelectric Nanogenerator Device

The piezoelectric nanogenerator devices based on CA/CNC nanocomposite membrane were manufactured with a typical sandwiched structure. A rectangular piece of CA/CNC nanocomposite membrane(3 cm×3 cm) was placed between two Cu tape electrodes(2 cm×2 cm). Each Cu tape electrode possessed a 0.5 cm strip to connect the external circuit. To avoid contamination during the measurements, the piezoelectric nanogenerator device was packaged well using one-side adhesive PET films(4 cm×4 cm, the thickness of 50 μm). To avoid the triboelectric effect, the gaps among the electrospun membrane, Cu tape electrodes, and PET films need to be eliminated by squeezing the device with proper pressure.

2.4 Characterization

The morphologies of nanofibers were observed by field emission scanning electron microscopy(FE-SEM, FEI Nova Nano 450). The crystal structure was determined by means of X-ray diffraction(XRD, PAN-PANalytical B.V. Empyrean) with Cu $K\alpha$ as the emission source. IR spectra of the samples were obtained on a Fourier transform infrared spectrometer(FTIR, Thermo Fisher Scientific iS10) using the KBr compression method at room temperature.

2.5 Measurement of Piezoelectric Performance

The voltage outputs of the device were recorded by an oscilloscope(OWON XDS3102A). A voice coil motor(Shenzhen Dongfang Servo Technology Co., Ltd., LA 15) driven by an AC servo driver(PD-B0409A) was used to apply the pressure to the devices. The pressure was measured by a multi-channel film pressure sensor(RFP ZQ-01).

3 Results and Discussion

In this work, CA and CA/CNC nanofiber membranes were prepared through the electrospinning technique. Fig.1(A) shows the electrospinning apparatus for producing nanofiber membranes. The morphology of CA and CA/CNC composite electrospun nanofibers was characterized by SEM. The surface of neat CA nanofibers is smooth without any polymer beads, and these nanofibers are randomly oriented[Fig.1(B)]. Moreover,

https://doi.org/10.1007/s40242-021-1252-x

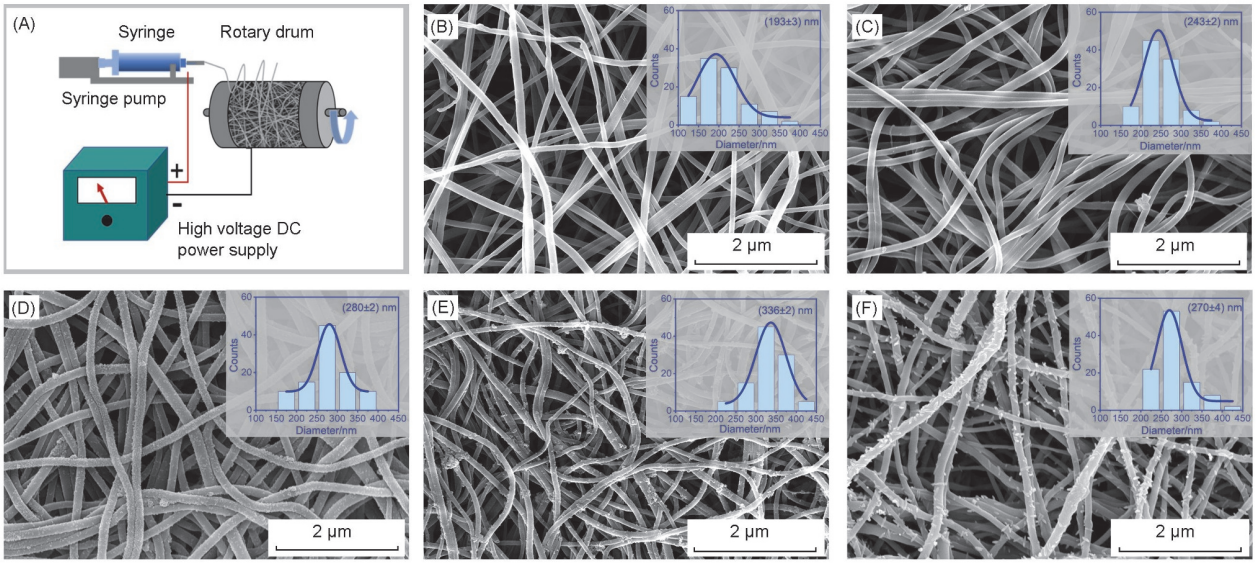

Fig.1 Schematic illustration of electrospinning apparatus(A), SEM images and fiber diameter distribution diagrams(insets) of electrospun nanofibers of CA(B), CA/CNC-5%(C), CA/CNC-10%(D), CA/CNC-15%(E), and CA/CNC-20%(F)

the diameter distribution diagrams of neat CA nanofibers and CA/CNC composite nanofibers with different amounts of CNC are also presented as the insets in Fig.1(B)—(F). With the increase of CNC content, the surface of the nanofiber became rough, because some nanocrystal rods appeared on the surface of nanofibers. The mean diameter of the CA/CNC composite nanofiber increases at first with the increasing amount of CNC and then slightly decreases. It is because that the increased amount of nanofiller will increase the diameter of fibers firstly, nevertheless, the abundant hydroxyl groups on the surface of CNC will also increase the degree of polarization of the solution, leading to the decrease of the diameter of the fibers[36,43,44].

To determine the crystallization in the composite nanofibers, the XRD patterns of the CA, CNC, and CA/CNC composite were carried out as shown in Fig.2(A). The XRD patterns of the CA nanofibers showed no obvious peak, indicating its low crystallinity. The XRD patterns of the CNC showed obvious peaks at 2θ = 22.5° and 34.4° corresponding to the (200) and (004) lattice plane of cellulose I[45]. In addition, there are two overlapping peaks at 2θ=15.5°, corresponding to the lattice plane of (101) and ($10\bar{1}$) cellulose type I crystal structure[46]. The XRD patterns of CA/CNC nanofibers showed similar peaks of CNC, indicating the existence of cellulose type I crystal structure in the composite nanofibers. Under the external force, the electric dipoles in the cellulose type I lattice can shift or reorient, resulting in the piezoelectric effect.

The FTIR spectra of the produced CA, CNC, and CA/CNC composite nanofibrous membranes are shown in Fig.2(B). Peaks at 2800—3000 cm^{-1}(stretching vibrations of C—H in —CH_2— groups), 1750 cm^{-1}(stretching vibration of C═O in acetyl and carboxylic acid), 1440 cm^{-1}(in-plane bending of —CH_2— or —OH), 1376 cm^{-1}(deformation of C—H in —CH_3), 1233 cm^{-1} (stretching of C—O in acetyl group), 1155 cm^{-1}(anti-symmetric bridge stretching of C—O—C), 1036 cm^{-1}(C—O—C of ether linkage of the glycosidic unit) and 883 cm^{-1}(β glycosidic linkages between the sugar units) can be observed in the spectra curves[47,48].

Fig.3(A) schematically illustrates the piezoelectric device structure based on the nanofibrous membranes. The piezoelectric generator consists of two copper foil electrodes on the top and bottom of the nanofiber membrane. The schematical

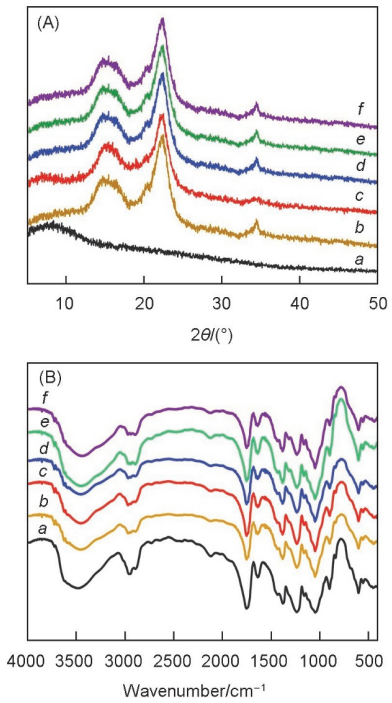

Fig.2 XRD patterns(A) and FTIR spectra(B) of CA nanofibers, CNC powder, and CA/CNC composite nanofibers

a. CA; *b*. CNC; *c*. CA/CNC-5%; *d*. CA/CNC-10%; *e*. CA/CNC-15%; *f*. CA/CNC-20%.

https://doi.org/10.1007/s40242-021-1252-x

illustration of the test apparatus is displayed in Fig.3(B). To investigate the piezoelectric properties, firstly, the device was fixed on a stable plane, and then both electrodes were connected to an oscilloscope. A periodic impacting-releasing force was applied perpendicularly on the top surface of the device. The electrical signals converted by the nanogenerator from mechanical energy were detected and recorded by the oscilloscope. The resultant piezoelectric output of the nanofiber piezoelectric generators under repeating pressing and releasing force of 5 N with the frequency of 2 Hz is presented in Fig.3(C). All the samples demonstrated the typical piezoelectric response when they underwent a periodic pressing-releasing force. Two opposite voltage signals are generated when the membrane was subjected to compression deformation and deformation disappearance, forming a signal pair like the alternating voltage, which could be explained detailedly in Fig.4. Initially, there is no piezoelectric output on the nanogenerator without any impact or vibration. The electric dipoles within the crystals are randomly distributed, resulting in a macroscopic electroneutrality in the electrospun fibers[Fig.4(A)]. When a vertical mechanical impact force was subjected to the device, a positive electrical signal was observed. The crystals in the nanofibers were compressed by the force and polarized, forming a potential difference between the two electrodes, and generating a flow of electrons in the external circuit[Fig.4(B)]. On the contrary, when the force was released, the device is recovered from the deformation and the electrons flew backward in the external circuit, thus generated a negative electrical signal[Fig.4(C)]. Moreover, it is noted that the voltage value of the positive peak is always greater than that of the negative peak, mainly due to the difference in the deformation rate for the material during the compressing and releasing process. In Fig.3(C), the output voltage is significantly improved with the involvement of CNC fillers. With the increase of CNC

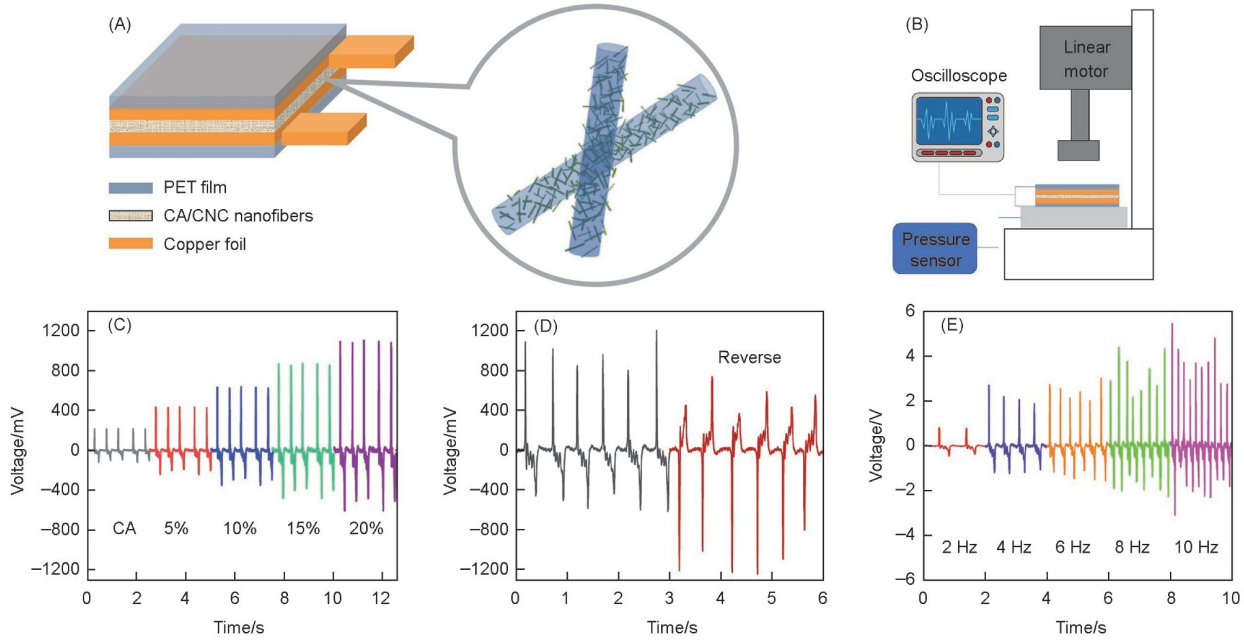

Fig.3 Schematical illustrations of the piezoelectric device structure(A) and the test apparatus(B), output voltages of CA and CA/CNC piezoelectric nanogenerators with different contents of CNCs under the impact force of 5 N at the frequency of 2 Hz(C), the output voltages of CA/CNC-20% piezoelectric nanogenerator device at forwarding connection and reverse connection(D), and the relationship of the frequency on open-circuit voltages under the impact force of 5 N on CA/CNC-20% piezoelectric nanogenerator device(E)

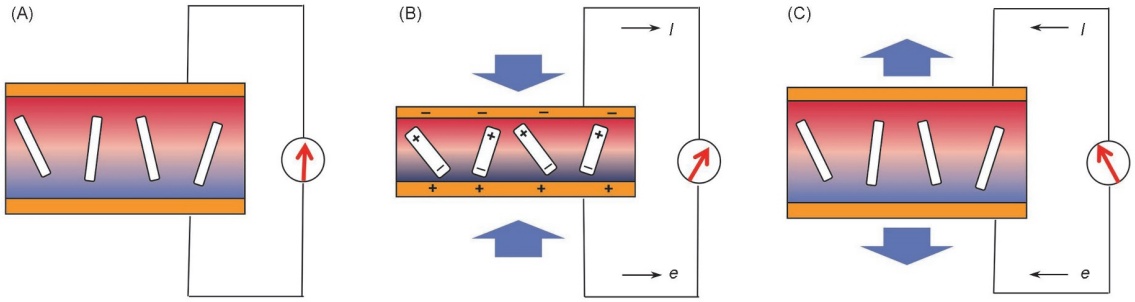

Fig.4 Principles of piezoelectric output in the impacting-releasing mode of nanofiber membrane piezoelectric nanogenerators
(A) No impacting; (B) impacting; (C) releasing.

https://doi.org/10.1007/s40242-021-1252-x

content, the output voltage of the nanogenerator also increases obviously. Under the repeated pressure of 5 N(frequency of 2 Hz), the nanogenerator device based on CA/CNC-20% can yield an electrical output of 1.2 V. Obviously, the addition of CNC could enhance the content of piezoelectric cellulose type I crystal. Furthermore, the mechanical properties of the nanocomposite membrane could also be improved because the local stress of the nanofiber is enhanced drastically by the rigidity of CNC rods, which would be beneficial for the reversion after the compress.

The output voltages of CA/CNC-20% piezoelectric nanogenerator device at forwarding connection and reverse connection under the impact force of 5 N at a frequency of 2 Hz were measured as shown in Fig.3(D). The amplitudes of the output signals under a reverse connection were almost the same as the ones under a forward connection, though the polarities of the signals were reversed, indicating that the obtained signals were piezoelectric outputs, rather than triboelectric outputs.

In addition, the relationship of the frequency on open-circuit voltages was also studied under an impact force of 5 N on CA/CNC-20% piezoelectric device[Fig.3(E)]. The voltage increased with the mechanical impacting frequency. The relationship between the piezoelectric outputs and the applied frequency should be attributed to that the increasing frequency could induce a faster strain rate of the piezoelectric fibers[49].

The peak voltages(U) and currents(I) of CA nanogenerator and CA/CNC-20% nanogenerator have been tested as the external loads increase from 20 kΩ to 6 MΩ under the impact force of 5 N at a frequency of 2 Hz, and the results are shown in Fig.5. It can be observed in Fig.5(A) and (C) that voltage outputs increased along with the increasing external resistance, in contrast, the current outputs presented an opposite trend. On the other hand, the instantaneous output power(P) at different external resistances, calculated by the equation: $P = UI$, first rose in the low resistance range, then fell in the high resistance range as shown in Fig.5(B) and (D). It is known that a power generator has the maximum power output when the external resistance is equivalent to the internal resistance of the device and that external resistance is called the optimum load. The maximum output power of the CA/CNC-20% nanogenerator was 0.625 μW when the external resistance was 1.08 MΩ. And the output power density is maximized at 0.156 μW/cm^2. Compared with CA/CNC-20% nanogenerator, the CA nanogenerator exhibits a lower maximum output power of 0.081 μW with a smaller internal resistance of 89 kΩ. This indicates that the addition of CNC is conducive to improving the output voltage of the external circuit, which could provide more electricity to the electrical appliances.

When the forces with different intensities were applied to CA/CNC-20% nanogenerator device, the output voltage increased obviously as the force increased. It is found the fitting of voltage outputs of CA/CNC-20% nanogenerator device to the force exhibits linear piezoelectricity as shown in Fig.6(A) and satisfies the linear relationship about y=0.248x+0.187. The sensitivity of the CA/CNC-20% nanogenerator device is 0.248 V/N with the applied force down to 2 N. Comparably, the voltage output of CA and force satisfy the linear relationship about y=0.05x+0.129, and the sensitivity is merely 0.05 V/N.

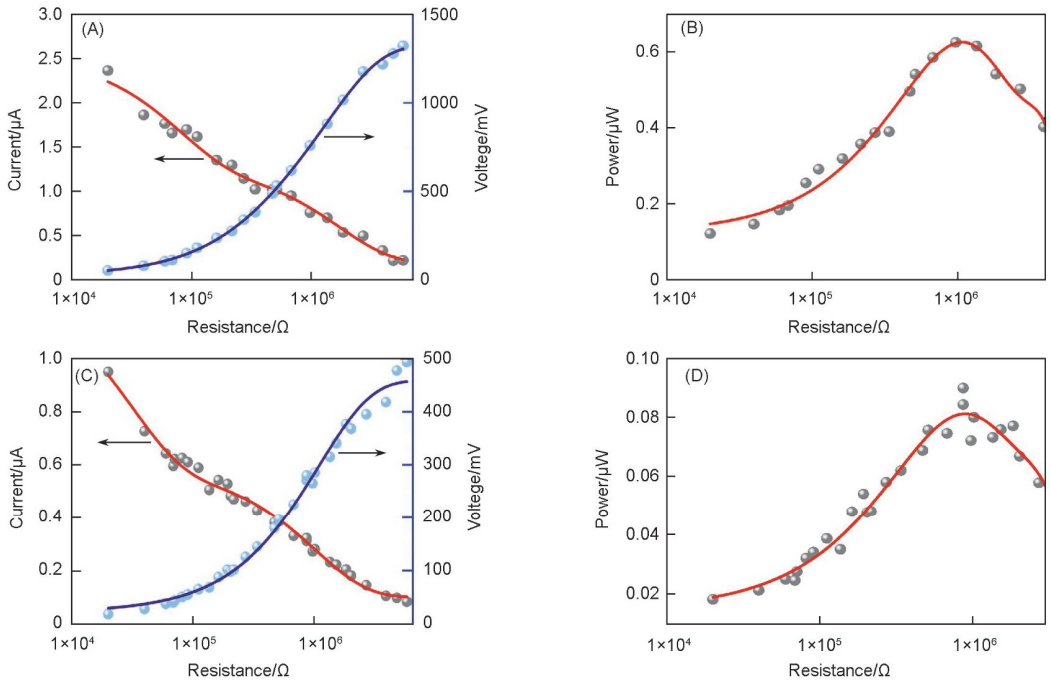

Fig.5 Peak voltage and current output change(A, C) and power output change(B, D) with an external load resistance of CA/CNC-20%(A, B) and CA nanogenerator devices(C, D) under the compressive impact of 5 N(frequency of 2 Hz)

https://doi.org/10.1007/s40242-021-1252-x

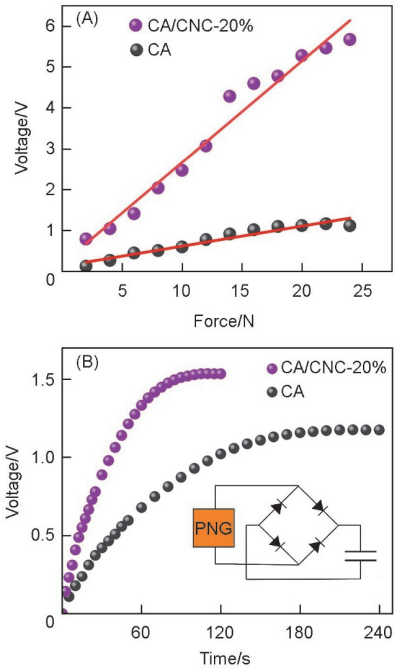

Fig.6 Voltage output of CA and CA/CNC-20% nanogenerator devices at different impact intensities(A) and charging curve of a commercial capacitor by CA and CA/CNC-20% nanogenerator devices under the compressive impact of 5 N(frequency of 2 Hz)(B)

Obviously, the CA/CNC-20% nanogenerator device possessed enhanced voltage outputs and sensitivity. Compared with the CA nanogenerator, when the CA/CNC-20% nanogenerator was compressed, the totally spontaneous polarization of the membrane is increased due to the increased content of piezoelectric cellulose type I crystal as the spontaneous polarization is proportional to the dipole moment per unit volume, and the local deformation of nanofibers is strengthened induced by the rigid nanorods[50]. Moreover, it suggests that the CA/CNC-20% nanogenerator shows a promising application in various fields, such as pressure sensors and health monitoring. Furthermore, the CA/CNC-20% nanogenerator device was connected to a commercial capacitor(10 μF) *via* a bridge rectifier. The electric power generated under the repeated compressive impact of 5 N could be collected effectively by the capacitor. As shown in Fig.6(B), the capacitor can be charged to 1.5 V in 2 min through the CA/CNC-20% nanogenerator device. However, it takes 4 min to charge the same commercial capacitor for the CA nanogenerator device. And the voltage of the commercial capacitor charged by CA nanogenerator device can reach only 1.2 V. The CA/CNC-20% nanogenerator device indicates a better potential in a self-supplying power source.

4 Conclusions

CA/CNC composite nanofiber membrane prepared by electrospinning method was utilized to fabricate a pressure-driven nanogenerator. The involvement of CNC increased the content of piezoelectric cellulose type I crystallization, and strengthened the mechanical properties of the nanofiber membrane, which together enhanced its piezoelectric properties. The CA/CNC-20% composite nanofiber membrane displays the highest piezoelectric conversion performance, and the output voltage can reach up to 1.2 V at 5 N with the frequency of 2 Hz. In addition, the output voltage of the CA/CNC-20% nanogenerator device exhibits a good linear relationship with applied impact force, indicating the great potential in pressure sensors and a self-supplying power source.

Acknowledgements

This work was supported by the National Natural Science Foundation of China (No.21875084).

Conflicts of Interest

The authors declare no conflicts of interest.

References

[1] Rodrigues C., Nunes D., Clemente D., Mathias N., Correia J. M., Rosa-Santos P., Taveira-Pinto F., Morais T., Pereira A., Ventura J., *Energy & Environmental Science*, **2020**, *13*(9), 2657
[2] Li L., Chen S., Wang X., Bando Y., Golberg D., *Energy & Environmental Science*, **2012**, *5*(3), 6040
[3] Liu G. H., Chen T., Xu J. L., Wang K. Y., *Journal of Materials Chemistry A*, **2018**, *6*(38), 18357
[4] Fu X. P., Bu T. Z., Li C. L., Liu G. X., Zhang C., *Nanoscale*, **2020**, *12*(47), 23929
[5] Ryu H., Yoon H. J., Kim S. W., *Advanced Materials*, **2019**, *31*(34), 1802898
[6] Chen J., Wang Z. L., *Joule*, **2017**, *1*(3), 480
[7] Kim H. S., Kim J. H., Kim J., *International Journal of Precision Engineering and Manufacturing*, **2011**, *12*(6), 1129
[8] Covaci C., Gontean A., *Sensors(Basel)*, **2020**, *20*(12), 3512
[9] Fan F. R., Tang W., Wang Z. L., *Adv. Mater.*, **2016**, *28*(22), 4283
[10] Wang Z. L., Song J. H., *Science*, **2006**, *312*(5771), 242
[11] Briscoe J., Dunn S., *Nano Energy*, **2015**, *14*, 15
[12] Kim J., Lee J. H., Ryu H., Lee J.-H., Khan U., Kim H., Kwak S. S., Kim S.-W., *Adv. Funct. Mater.*, **2017**, *27*(22), 1700702
[13] Costa P., Nunes-Pereira J., Pereira N., Castro N., Goncalves S., Lanceros-Mendez S., *Energy Technology*, **2019**, *7*(7), 1800852
[14] Zhang H., Yang Y., Su Y., Chen J., Adams K., Lee S., Hu C., Wang Z. L., *Adv. Funct. Mater.*, **2014**, *24*(10), 1401
[15] Wang Z. L., *ACS Nano*, **2013**, *7*(11), 9533
[16] Liu X., Cui P., Wang J., Shang W., Zhang S., Guo J., Gu G., Zhang B., Cheng G., Du Z., *Nanotechnology*, **2021**, *32*(7), 075401
[17] Wang X., *Nano Energy*, **2012**, *1*(1), 13
[18] Siddiqui S., Kim D.-I., Duy L. T., Nguyen M. T., Muhammad S., Yoon W.-S., Lee N.-E., *Nano Energy*, **2015**, *15*, 177
[19] Li Z., Zheng Q., Wang Z. L., Li Z., *Research(Wash D C)*, **2020**, 8710686
[20] Hasan M. R., Baek S. H., Seong K. S., Kim J. H., Park I. K., *ACS Appl. Mater. Interfaces*, **2015**, *7*(10), 5768
[21] Le A. T., Ahmadipour M., Pung S.-Y., *Journal of Alloys and Compounds*, **2020**, *844*, 156172
[22] Chen X., Xu S., Yao N., Shi Y., *Nano Lett.*, **2010**, *10*(6), 2133
[23] Park K. I., Son J. H., Hwang G. T., Jeong C. K., Ryu J., Koo M., Choi I., Lee S. H., Byun M., Wang Z. L., Lee K., *J. Adv. Mater.*, **2014**, *26*(16), 2514
[24] Ni X., Wang F., Lin A., Xu Q., Yang Z., Qin Y., *Science of Advanced Materials*, **2013**, *5*(11), 1781
[25] Shirazi P., Ico G., Anderson C. S., Ma M. C., Kim B. S., Nam J., Myung N. V., *Advanced Sustainable Systems*, **2017**, *1*(11), 1700091
[26] Kalimuldina G., Turdakyn N., Abay I., Medeubayev A., Nurpeissova A., Adair D., Bakenov Z., *Sensors(Basel)*, **2020**, *20*(18), 5214
[27] Yan J., Liu M., Jeong Y. G., Kang W., Li L., Zhao Y., Deng N., Cheng B., Yang G., *Nano Energy*, **2019**, *56*, 662
[28] Song Y. H., Shi Z. Q., Hu G. H., Xiong C. X., Isogai A., Yang Q. L., *Journal*

of Materials Chemistry A, **2021**, *9*(4), 1910
[29] Moon R. J., Martini A., Nairn J., Simonsen J., Youngblood J., *Chemical Society Reviews*, **2011**, *40*(7), 3941
[30] Fukada E., *Ultrasonics*, **1968**, *6*(4), 229
[31] Nakai T., Yamamoto H., *Holzforschung*, **2007**, *61*(1), 95
[32] Zhao D., Zhu Y., Cheng W., Chen W., Wu Y., Yu H., *Adv. Mater.*, **2020**, 2000619
[33] Hirai N., Sobue N., Date M., *Journal of Wood Science*, **2011**, *57*(1), 1
[34] Zheng Q., Zhang H., Mi H., Cai Z., Ma Z., Gong S., *Nano Energy*, **2016**, *26*, 504
[35] Wu T., Song Y., Shi Z., Liu D., Chen S., Xiong C., Yang Q., *Nano Energy*, **2021**, *80*, 105541
[36] Fashandi H., Abolhasani M. M., Sandoghdar P., Zohdi N., Li Q. X., Naebe M., *Cellulose*, **2016**, *23*(6), 3625
[37] Wang J., Carlos C., Zhang Z., Li J., Long Y., Yang F., Dong Y., Qiu X., Qian Y., Wang X., *ACS Appl. Mater. Interfaces*, **2020**, *12*(23), 26399
[38] Annamalai P. K., Nanjundan A. K., Dubal D. P., Baek J. B., *Advanced Materials Technologies*, **2021**, *6*(3), 2001164
[39] Lasrado D., Ahankari S., Kar K., *Journal of Applied Polymer Science*, **2020**, *137*(27), 48959
[40] Cui P., Parida K., Lin M.-F., Xiong J., Cai G., Lee P. S., *Advanced Materials Interfaces*, **2017**, *4*(22), 1700651
[41] Wang J., Carlos C., Zhang Z., Li J., Long Y., Yang F., Dong Y., Qiu X., Qian Y., Wang X., *ACS. Applied Materials & Interfaces*, **2020**, *12*(23), 26399
[42] Hänninen A., Sarlin E., Lyyra I., Salpavaara T., Kellomaki M., Tuukkanen S., *Carbohydrate Polymers*, **2018**, *202*, 418
[43] Nair S. S., Mathew A. P., *Carbohydrate Polymers*, **2017**, *175*, 149
[44] Ni X. H., Cheng W. L., Huan S. Q., Wang D., Han G. P., *Carbohydrate Polymers*, **2019**, *206*, 29
[45] Rojanarata T., Plianwong S., Su-Uta K., Opanasopit P., Ngawhirunpat T., *Talanta*, **2013**, *115*, 208
[46] Xie Y. L., Wang M. J., Yao S. J., *Langmuir*, **2009**, *25*(16), 8999
[47] Song W., Liu D., Prempeh N., Song R., *Biomacromolecules*, **2017**, *18*(10), 3273
[48] Chen J., Xu J., Wang K., Cao X., Sun R., *Carbohydr Polym*, **2016**, *137*, 685
[49] Shi K. M., Sun B., Huang X. Y., Jiang P. K., *Nano Energy*, **2018**, *52*, 153
[50] Jiang J., Tu S., Fu R., Li J., Hu F., Yan B., Gu Y., Chen S., *ACS Appl. Mater. Interfaces*, **2020**, *12*(30), 33989